Materials Letters 306 (2022) 130924

Contents lists available at ScienceDirect

Materials Letters

journal homepage: www.elsevier.com/locate/matlet

Aerosol deposition of anode functional layer for metal-supported solid oxide fuel cells

I.S. Erilin [a], I.N. Burmistrov [a,b], D.A. Agarkov [a,b], E.A. Agarkova [a], D.V. Yalovenko [a], A. A. Solovyev [c,*], S.V. Rabotkin [c], V.E. Pukha [d], N.V. Lyskov [d], S.I. Bredikhin [a,b]

[a] Osipyan Institute of Solid State Physics RAS, Chernogolovka, Moscow District 142432, Russia
[b] Moscow Institute of Physics and Technology, Dolgoprudny, Moscow District 141701, Russia
[c] Institute of High Current Electronics SB RAS, Tomsk 634055, Russia
[d] Institute of Problems of Chemical Physics RAS, Chernogolovka, Moscow District 142432, Russia

ARTICLE INFO

Keywords:
Aerosol deposition
Metal-supported solid oxide cell
Anode
MS-SOFC
MS-SOEC

ABSTRACT

In order to increase efficiency of metal-supported solid oxide fuel cells (SOFCs) and electrolysis cells (SOECs) and to lower their fabrication and operation temperatures, development of novel methods for the functional layers deposition is of primary importance. In this work, the composite anodes of metal-supported solid oxide cells (MS-SOCs), made of Ni and 10 mol.% scandia and 1 mol.% yttria co-stabilized zirconia (10Sc1YSZ), were deposited by the aerosol deposition (AD) onto high relief porous metal substrates. This step was followed by magnetron sputtering (MSP) of thin 8 mol.% yttria-stabilized zirconia (8YSZ) solid electrolyte. Vacuum co-sintering of the half-cells at 1100 °C resulted in the formation of well-bonded nanostructured anodes and gas-tight electrolyte membranes. The area-specific ohmic resistance of the half-cell in dry hydrogen was 0.23 Ohm·cm^2 at 577 °C.

1. Introduction

Metal-supported solid oxide electrochemical cells are the next-generation SOCs consisting of all-thin-film functional layers and porous metal support. MS-SOCs provide several advantages with respect to ceramic-supported SOCs, such as thermal cycling tolerance, mechanical strength, and the fast startup [1]. The necessity to operate MS-SOCs in the temperature range below 650 °C [2] results in a significant reduction of costs for the SOCs stacks and energy systems [3] but, on the other hand, entails the use of advanced film-deposition techniques [4].

One of the major problems in the MS-SOC production is related to the formation of an anode functional layer due to the challenging relief and easily oxidizable nature of the metal support, as well as coarsening of deposited Ni during sintering of the anode at elevated temperatures [5]. In the present work, the aerosol deposition method was used in order to form nanostructured composite anodes for MS-SOCs with high-relief porous metal supports. The AD method gives an opportunity to deposit thin [6] or thick [7] gas-tight [8] or porous [9] layers at low vacuum (1–1000 Pa) and room temperature.

2. Experimental section

The AD equipment used in this work was described elsewhere [8,10]. The aerosol jet was formed using a 0.5 mm^2 converging nozzle with axial symmetry. Nitrogen was used as a carrier gas. The angle between the nozzle and substrate during anode deposition onto the porous metal substrates was chosen equal to 90°, which corresponds to a direct impact of the aerosol jet on the substrate. The absolute pressures in the deposition chamber and in front of the nozzle were 200–400 Pa and 0.2–0.3 MPa, respectively.

Analysis of the anode formation by the AD method was carried out with three different composite powders listed in Table 1.

Ball-milling of the composites was carried out using Pulverisette 6 classic line ball mill (Fritsch, Germany). The anode layers were deposited onto porous metal disks made of X17H2 [11] steel powder produced by Polema, JSC (Russia). The disks were compacted by uniaxial pressing followed by sintering in a vacuum furnace at 1100 °C. 8YSZ thin films were deposited by MSP [12] on the substrates with as-deposited unsintered anodes. Sintering of the metal-supported cells with deposited anodes and co-sintering of the electrolyte and anode was carried out at 1100 °C for 1 h in a vacuum furnace (ThermoCeramics, Russia).

* Corresponding author.
E-mail address: andrewsol@mail.ru (A.A. Solovyev).

https://doi.org/10.1016/j.matlet.2021.130924
Received 10 September 2021; Received in revised form 16 September 2021; Accepted 18 September 2021
Available online 22 September 2021

Table 1
Composition and preparation of the anode powders.

Designation	Composition*	Preparation
Composite-1	NiO/10Sc1YSZ = 60/40 vol%	annealing at 700 °C, milling by 10 mm stabilized zirconia balls at the speed of 400 rpm
Composite-2	NiO/10Sc1YSZ = 60/40 vol%	no annealing, milling by 10 mm balls at 400 rpm
Composite-3	Ni/10Sc1YSZ = 50/50 vol%	no annealing, roll-milling at 35 rpm

* NiO (Sigma Aldrich, USA), 10Sc1YSZ (Qingdao Terio Corp., China), Ni (IEP UB RAS, Russia).

Microstructure of the anodes and half-cells before and after sintering was examined using scanning electron microscopy (SEM, Supra 50VP, Zeiss, Germany). Transport properties of the half-cells in flowing dry hydrogen were studied by the impedance spectroscopy (1260A, Solartron, UK) using Ag electrical contacts. The silver contacts were applied onto the electrolyte and metal substrate surfaces, followed by drying in air without extra thermal treatments.

3. Results and discussion

The SOC anodes should have a sufficient porosity for fuel supply, a well-bonded microstructure, and an extended triple-phase boundary for fast kinetics of the electrochemical reactions. Fig. 1 displays SEM images of the composite anode surfaces after AD. The deposition of Composite-1 (Fig. 1a and 1b) leads to partial closing of the substrate pores; furthermore, there are traces of metal surface erosion. Composite-2 (Fig. 1c–d) evenly covers the substrate surface and partially fills its pores. The deposition of Composite-3 (Fig. 1e–f) results in full covering of the substrate and fills all pores. As the even coverage of the metal substrate is important for the SOC performance, analysis of the sintered anode microstructures was only conducted in two latter cases.

Fig. 2 shows surfaces of Composites 2 and 3 after sintering at 1100 °C in vacuum. The layer of Composite-2 (Fig. 2a–b) becomes Ni-depleted due to NiO reduction and consequent diffusion of Ni into the metal substrate. The resultant layer consists of the bare 10Sc1YSZ skeleton partially incorporated into the metal substrate. Composite-3 (Fig. 2c–f) provided a complete coverage of the metal substrate even after sintering. The high-resolution secondary electrons image (Fig. 2e) shows a well-bonded porous structure of the sintered layer; the back-scatter SEM image (Fig. 2f) indicates a uniform distribution of Ni (dark) and 10Sc1YSZ (bright) phases. In other words, the increased amount of Ni in Composite-3 results in the homogeneous well-bonded anode with an extended triple-phase boundaries and a good coverage of the metal substrate. The flat and low-relief surface of Composite-3 anode is a good base for electrolyte deposition by MSP [13].

The anode layers made using Composite-3 were, therefore, used for the solid electrolyte film deposition. Fig. 3 presents SEM images of the resulting half-cell before (a–c) and after co-sintering at 1100 °C (d). The sputtered electrolyte layer (Fig. 3a,b) possesses a columnar structure without any cracks and major defects. The half-cell cross-section (Fig. 3b) reveals a nanostructured anode with a thickness of approximately 30 μm and a thin (~4 μm) crack-free electrolyte. In order to obtain a porous well-bonded anode and to consolidate the electrolyte film, the co-sintering procedure was carried out. The columnar structure (Fig. 3c) appearing due to oxygen deficiency in the electrolyte layer deposited by MSP, was essentially eliminated after vacuum sintering (Fig. 3d). The sintered half-cell exhibits a well-developed porosity and

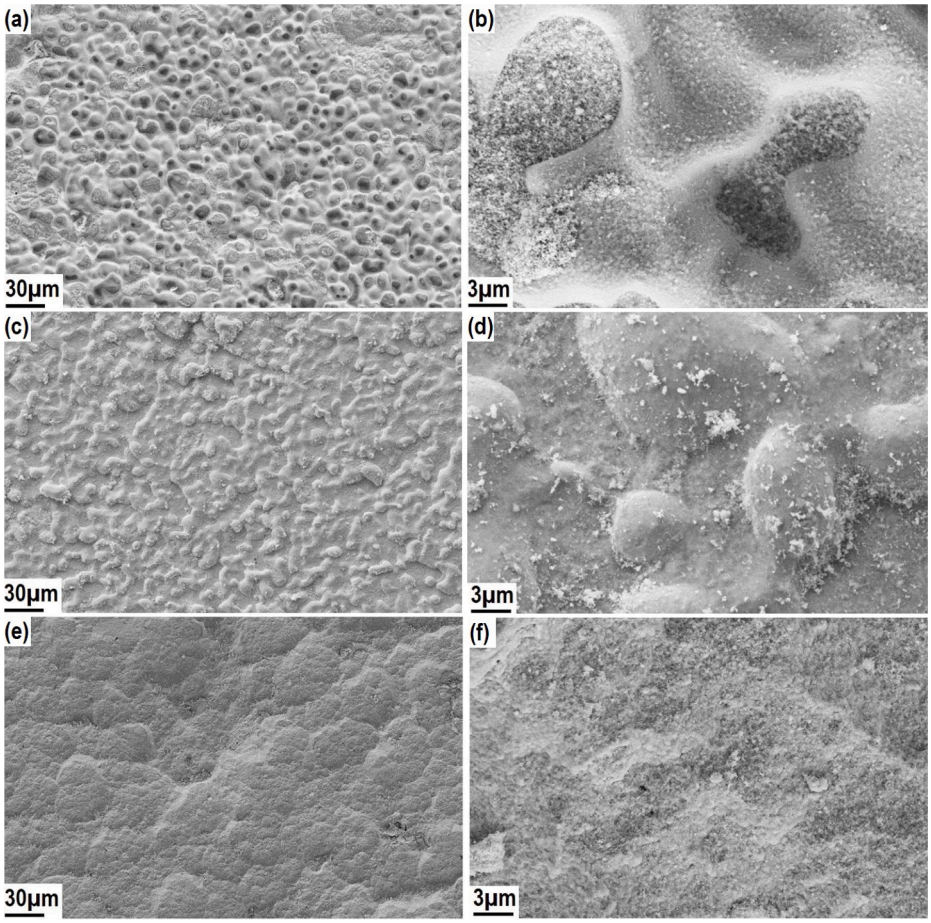

Fig. 1. SEM images of the surfaces of Composite-1 (a–b), Composite-2 (c–d), and Composite-3 (e–f) deposited on the porous metal substrates.

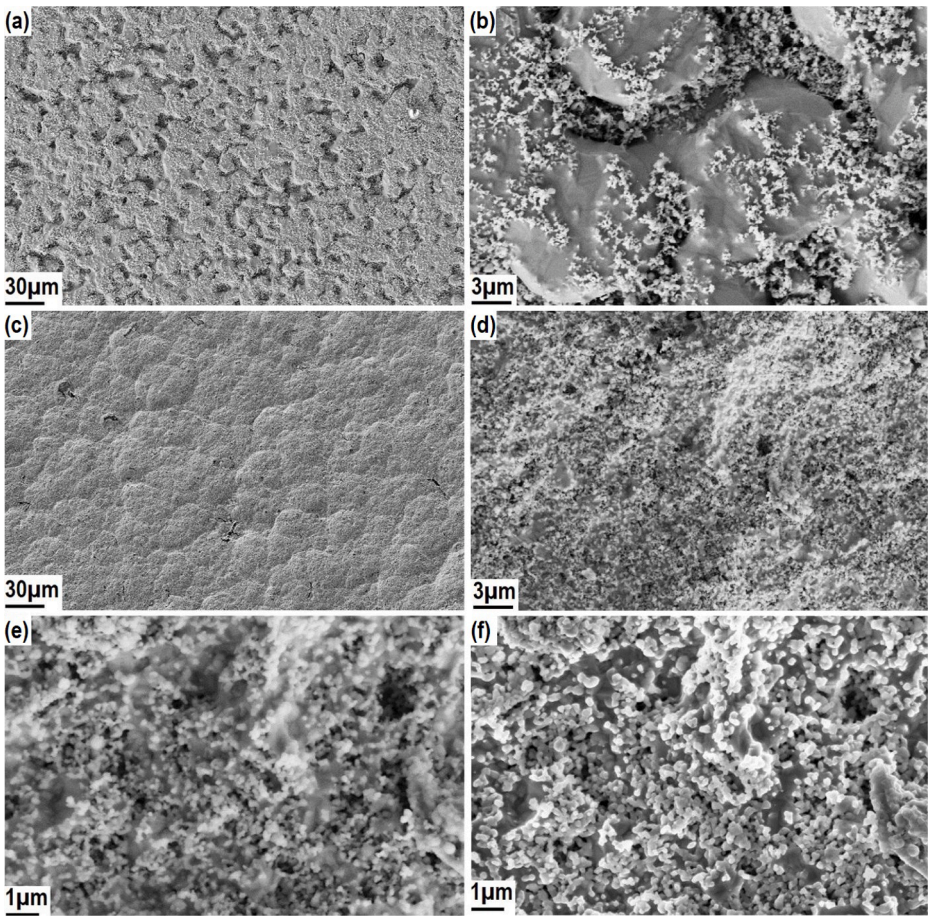

Fig. 2. SEM images of the surfaces of Composite-2 (a–b) and Composite-3 (c–f) anodes after sintering at 1100 °C from secondary electrons (a–e) and backscattered electrons detectors (f).

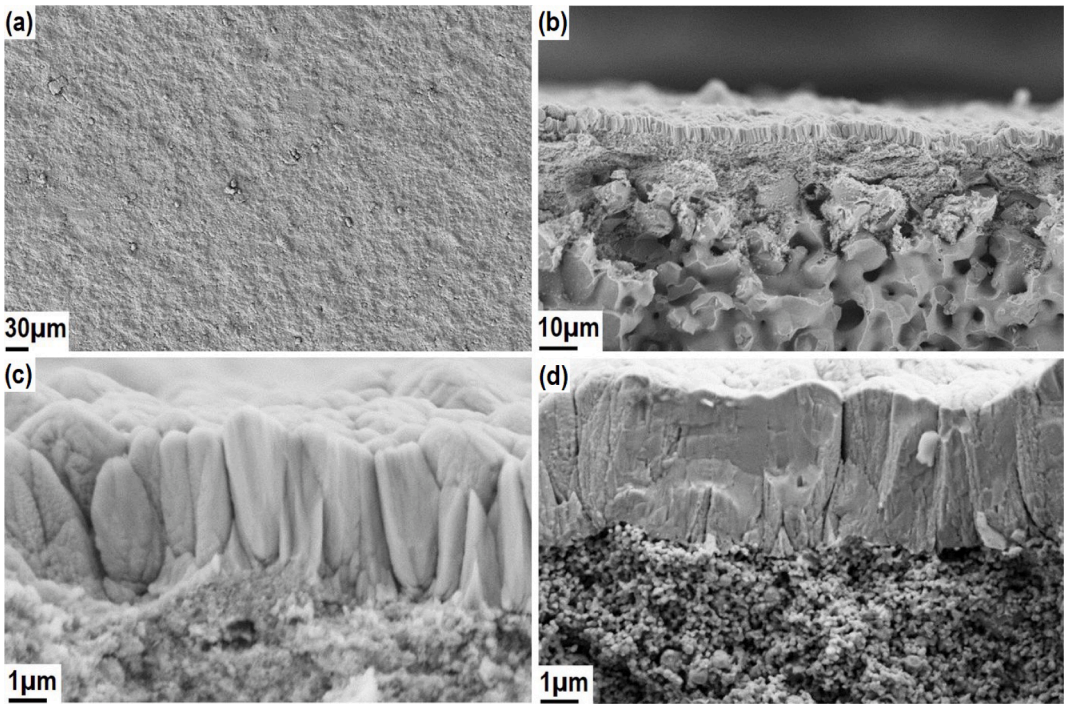

Fig. 3. Surface (a) and cross-section (b) of the half-cell after the deposition of anode by AD and electrolyte film by MSP, and high-magnification images of the anode and electrolyte layers before (c) and after vacuum co-sintering at 1100 °C (d).

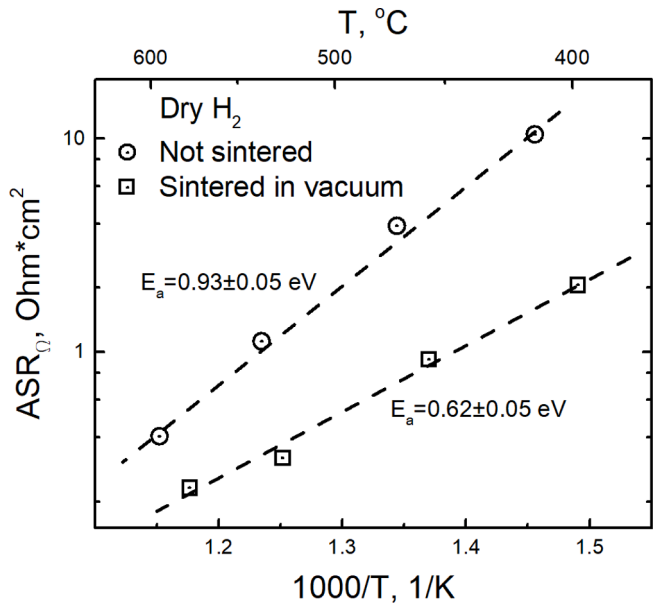

Fig. 4. Temperature dependence of the ASR_{Ω} for the half-cells before and after the sintering.

good adhesion between the layers.

Fig. 4 presents the Arrhenius dependencies of ohmic component of the area-specific resistance (ASR_{Ω}) extracted from the impedance spectra, for the half-cells after and before sintering. The activation energies are 0.93 eV and 0.62 eV for the green and sintered half-cells, respectively.

4. Conclusions

The nanostructured composite anodes for MS-SOCs were formed using the AD method. The full coverage of the high-relief porous metal substrate with good adhesion to the substrate were achieved for Composite-3 consisting of 50 vol% Ni and 50 vol% 10Sc1YSZ electrolyte. The MSP method was successfully used for the subsequent deposition of thin electrolyte layer on the unsintered anode. The vacuum co-sintering of the half-cells at 1100 °C made it possible to achieve sufficient mechanical strength and well developed interface between the anode and solid electrolyte, preserving porous structure of the anode. The ohmic ASR_{Ω} of the sintered half-cell was as low as 0.23 Ohm·cm^2 in a dry hydrogen atmosphere at 577 °C.

CRediT authorship contribution statement

I.S. Erilin: Data curation, Investigation, Writing – original draft. **I.N. Burmistrov:** Investigation, Methodology, Writing – original draft. **D.A. Agarkov:** Writing – original draft, Writing – review & editing. **E.A. Agarkova:** Data curation, Investigation. **D.V. Yalovenko:** Data curation, Investigation. **A.A. Solovyev:** Data curation, Investigation. **S.V. Rabotkin:** Data curation, Investigation. **V.E. Pukha:** Data curation, Investigation. **N.V. Lyskov:** Data curation, Investigation. **S.I. Bredikhin:** Supervision, Methodology.

Declaration of Competing Interest

The authors declare that they have no known competing financial interests or personal relationships that could have appeared to influence the work reported in this paper.

Acknowledgements

This work was financially supported by Ministry of Science and Higher Education of Russian Federation (unique identifier of the contract RFMEFI60819X0279, contract 05.608.21.0279); and by Nissan Research Division, Nissan Motor Co., Ltd.

References

[1] M.C. Tucker, Progress in metal-supported solid oxide fuel cells: A review, J. Power Sources 195 (15) (2010) 4570–4582, https://doi.org/10.1016/j.jpowsour.2010.02.035.
[2] T. Klemensø, J. Nielsen, P. Blennow, A. Persson, T. Stegk, P. Hjalmarsson, B. Christensen, S. SøNderby, J. Hjelm, S. Ramousse, Development of Long-Term Stable and High-Performing Metal-Supported SOFCs, ECS Trans. 35 (2019) 369–378, https://doi.org/10.1149/1.3570011.
[3] R.T. Leah, A. Bone, A. Selcuk, D. Corcoran, M. Lankin, Z. Dehaney-Steven, M. Selby, P. Whalen, Development of Highly Robust, Volume-Manufacturable Metal-Supported SOFCs for Operation Below 600°, ECS Trans. 35 (2019) 351–367, https://doi.org/10.1149/1.3570010.
[4] J. Nielsen, Å.H. Persson, T.T. Muhl, K. Brodersen, Towards High Power Density Metal Supported Solid Oxide Fuel Cell for Mobile Applications, J. Electrochem. Soc. 165 (2) (2018) F90–F96, https://doi.org/10.1149/2.0741802jes.
[5] P. Blennow, J. Hjelm, T. Klemensø, S. Ramousse, A. Kromp, A. Leonide, A. Weber, Manufacturing and characterization of metal-supported solid oxide fuel cells, J. Power Sources 196 (17) (2011) 7117–7125, https://doi.org/10.1016/j.jpowsour.2010.08.088.
[6] I.S. Erilin, D.A. Agarkov, I.N. Burmistrov, V.E. Pukha, D.V. Yalovenko, N.V. Lyskov, M.N. Levin, S.I. Bredikhin, Aerosol deposition of thin-film solid electrolyte membranes for anode-supported solid oxide fuel cells, Mater. Lett. 266 (2020) 127439, https://doi.org/10.1016/j.matlet.2020.127439.
[7] J. Akedo, M. Lebedev, Microstructure and electrical properties of lead zirconate titanate (Pb(Zr52/Ti48)O3) thick films deposited by aerosol deposition method, Jpn. J. Appl. Phys. 38 (1999) 5397–5401, https://doi.org/10.1143/jjap.38.5397.
[8] I.S. Erilin, I.N. Burmistrov, D.A. Agarkov, V.E. Pukha, D.V. Yalovenko, N.V. Lyskov, M.N. Levin, S.I. Bredikhin, Aerosol deposition of thin-film single- and bi-layered solid electrolytes for intermediate temperature planar solid oxide fuel cells, ECS Trans. 103 (1) (2021) 1695–1703, https://doi.org/10.1149/10301.1695ecst.
[9] J. Ryu, B.-D. Hahn, J.-J. Choi, W.-H. Yoon, B.-K. Lee, J.H. Choi, D.-S. Park, Porous photocatalytic TiO2 thin films by aerosol deposition, J. Am. Ceram. Soc. 93 (2010) 55–58, https://doi.org/10.1111/j.1551-2916.2009.03391.x.
[10] S.I. Bredikhin, D.A. Agarkov, E. Agarkova, I. Burmistrov, A. Cherkasov, V. Pukha, D. Yalovenko, N. Lyskov, Aerosol deposition as a promising technique to fabricating a thin-film solid electrolyte of solid oxide fuel cells, ECS Trans. 91 (1) (2019) 403–413, https://doi.org/10.1149/09101.0403ecst.
[11] https://auremo.biz/materials/stal-h17n2.html Accessed 31 August 2021.
[12] A.A. Solovyev, A.V. Shipilova, I.V. Ionov, A.N. Kovalchuk, S.V. Rabotkin, V. O. Oskirko, Magnetron-sputtered YSZ and CGO electrolytes for SOFC, J. Electron. Mater. 45 (8) (2016) 3921–3928, https://doi.org/10.1007/s11664-016-4462-0.
[13] H. Wang, W. Ji, L. Zhang, Y. Gong, B. Xie, Y. Jiang, Y. Song, Preparation of YSZ films by magnetron sputtering for anode-supported SOFC, Solid State Ion. 192 (1) (2011) 413–418, https://doi.org/10.1016/j.ssi.2010.05.022.